Environmental and Experimental Botany 162 (2019) 504–514

Contents lists available at ScienceDirect

Environmental and Experimental Botany

journal homepage: www.elsevier.com/locate/envexpbot

Changes in growth and photosynthesis linked with intensity and duration of salinity in *Phragmites karka*

Erum Shoukat[a], Zainul Abideen[a], Muhammad Zaheer Ahmed[a,*], Salman Gulzar[a], Brent L. Nielsen[b]

[a] Institute of Sustainable Halophyte Utilization, University of Karachi, Karachi, 75270, Pakistan
[b] Department of Microbiology and Molecular Biology, Brigham Young University, Provo, UT, 84602, USA

ARTICLE INFO

Keywords:
Marshy grass
Oxidative damage
Photosynthetic pigments
Plant photochemistry
Stomatal limitation
Biochemical limitation

ABSTRACT

Phragmites karka is gaining increasing attention as a biofuel crop due to high ligno-cellulosic biomass. In this study we investigated plant growth, gas exchange, chlorophyll fluorescence, photosynthetic pigments, and soluble sugar after 7, 15, and 30 days exposure to saline conditions [0 (control), 100 mM (moderate) and 300 mM (high) NaCl treatments]. Growth rate and net photosynthesis (A_{NET}) were unchanged during short term (0–7 days) exposure to moderate salinity but decreased at 300 mM NaCl due to reduction in net assimilation rate, stomatal conductance (gs), and intercellular carbon dioxide concentration (Ci). However, growth rate decreased under long term (15–30 days) exposure to moderate salinity, while an increase in water use efficiency (WUE) and instantaneous carboxylation efficiency (COE) helped to maintain A_{NET}. Higher photosynthetic pigments, respiration, sugar content and efficiency of photosystem II (YII) appear to work together to reduce the risk of oxidative stress at 100 mM NaCl. Long term exposure at 300 mM NaCl decreased the A_{NET}, gs, COE, and YII. Stomatal closure improved WUE but resulted in increased ROS production (ETR/A_{gross}). Photosynthesis was reduced by stomatal limitation under short-term exposure to high salinity and by both stomatal and biochemical limitation during long term exposure. These results indicate that *P. karka* can survive in moderate salinity for long durations by photosynthetic adaptations (photochemistry and gas exchange) that are vital for growth and biomass production in natural ecosystems.

1. Introduction

Plant growth is linked with photosynthetic performance and changes in carbon economy under saline conditions (Gorai et al., 2011; Nackley and Kim, 2015; Webster et al., 2016; Asrar et al., 2017; Wungrampha et al., 2018). Salinity stress often results in biomass reduction as a survival strategy of plants which is related with failure in carbon assimilation (Nackley and Kim, 2015; Sanchez et al., 2016; Fall et al., 2017; Pompeiano et al., 2017). In such situations, plants distribute higher assimilated carbon to energy and maintenance rather than development of plant parts (Kumar et al., 2016; Asrar et al., 2017). One example of this is the production of stress protecting metabolites such as sugar, proline, polyphenols and others (Slama et al., 2015; Sami et al., 2016; Liang et al., 2018; Yang and Guo, 2018). Utilization and transport of soluble sugar helps the plant to alleviate the negative effects of salinity via osmotica, osmoprotectants or ROS scavengers and regulate photosynthesis through feedback inhibition (Dadkhah and Rassam, 2016; Sami et al., 2016).

Photosynthetic rates are reported to be linked with salinity concentration and duration of salt exposure (Liu et al., 2011; Rakhmankulova et al., 2016; Fall et al., 2017; Pompeiano et al., 2017). A decrease in net CO_2 assimilation is linked with stomatal closure to regulate transpiration rate and water use efficiency in the initial phase of salinity exposure (Hetherington and Woodward, 2003; Liu et al., 2011). Long term salinity alters biochemical reactions (like Rubisco carboxylase/oxygenase activity and regeneration of RuBP and triose

Abbreviations: A_{NET}, net photosynthetic rate; Ci, intercellular carbon dioxide concentration; COE, instantaneous carboxylation efficiency; E, transpiration; ETR, electron transport rate; Fv/Fm, maximum quantum yield of PS II; gs, Stomatal conductance; LAR, leaf area ratio; LMF, leaf mass fraction; NPQ, non photochemical quenching; P_R, photorespiration; qP, photochemical quenching; Rd, dark respiration; RGR, relative growth rate; SLA, specific leaf area; SS, soluble sugar; ULR, unit leaf rate; WUE, water use efficiency; Y(NO), quantum yield of non-regulated non-photochemical energy loss in PSII; Y(NPQ), quantum yield of regulated non-photochemical energy loss in PS II; YII, effective photochemical quantum yield of PS II

* Corresponding author.
E-mail address: mzahmed@uok.edu.pk (M.Z. Ahmed).

https://doi.org/10.1016/j.envexpbot.2019.03.024
Received 26 February 2019; Received in revised form 25 March 2019; Accepted 25 March 2019
Available online 26 March 2019
0098-8472/

phosphates) that regulate gas-exchange (Eller et al., 2014; Asrar et al., 2017). However, in some grasses both stomatal and biochemical limitation appear to affect photosynthesis as in the case of *Eremochloa ophiuroides* (Liu et al., 2011), *Aeluropus lagopoides* and *Sporobolus tremulus* (Moinuddin et al., 2017). Stomatal and biochemical limitation inhibit the utilization of ATP and NADH for CO_2 assimilation leading to photochemical limitation (Takahashi and Badger, 2011; Percey et al., 2016). This excess excitation energy causes an oxidative burst in chloroplasts that damage the photosynthetic apparatus, predominantly photosystem II (PSII), D_1 and D_2 proteins (Redondo-Gómez et al., 2007; Pang et al., 2010; Takahashi and Badger, 2011; Percey et al., 2016). Salinity impaired biosynthesis and/or accelerated degradation of photosynthetic pigments lead to photo-inhibition (Megdiche et al., 2008; Moinuddin et al., 2017). In general, halophytic grasses are reported to decrease chlorophyll content under salinity (Liu et al., 2011; Khalafallah et al., 2013; Asrar et al., 2017; Moinuddin et al., 2017). Grasses have evolved numerous photo-protective mechanisms including heat dissipation through the xanthophyll cycle, quenching of excess electrons at PSI, and preventing over-reduction of the electron transport chain by photorespiration (Asrar et al., 2017; Moinuddin et al., 2017).

Increasing trends in world population and demand for energy along with rapidly diminishing fossil fuel sources are emphasizing a needed switch to alternate solutions like biofuels (Shamsutdinov et al., 2017). At the same time, soil salinity causes heavy losses to prime land, which is a major constraint to realise the desired goals. It is estimated that food production will need to expand by 50–70% to fulfill the future requirements worldwide (Millar and Roots, 2012). In addition, the demand for biomass derived energy production through biofuel also increases the pressure on conventional agriculture. However, most biofuel crops are salt sensitive, and there has been a conflict between using land for producing feed or fuel (Abideen et al., 2011). A suitable option is thus to use salt resistant plants as second generation biofuel candidates (Abideen et al., 2011; Shamsutdinov et al., 2017).

Phragmites karka is considered as a potential candidate for biofuel because of suitable ligno-cellulosic content (Abideen et al., 2011), and high productivity (capable of growth up to 4–10 meter height: Flora of Pakistan, 2011). Biomass is linked directly with plant photosynthetic capacity but negatively influenced by soil salinity (Webster et al., 2016; Asrar et al., 2017; Wungrampha et al., 2018). Abideen et al. (2018) reported that *P. karka* maintained growth and net photosynthesis at 100 mM NaCl, whereas growth reduction under high salinity was due to stomatal closure and co-occuring reduction in CO_2 uptake. However, it still remains unclear whether the decrease in photosynthesis of *P. karka* is the reason or the result of growth reduction. Information is also lacking regarding the relationship of growth rate with photosynthetic efficiency of *P. karka* at different time intervals of saline condition. This information would be useful to decrease the energy and land crises by using saline degraded land. Therefore, the present study was designed to determine changes in growth and photosynthetic attributes of *P. karka* in response to salinity concentration and duration of salinity treatment.

2. Materials and methods

2.1. Experimental conditions and salinity treatment

Seeds of *Phragmites karka* were collected from marshy habitats of Karachi University, Pakistan (24°55′3″ N and 67°6′19″ E) in February 2014. Freshly collected seeds were sown in plastic trays containing sandy soil plus manure and irrigated with water for germination. Five week old seedlings of similar size (length 6–8 cm, three leaf stage) were transplanted into plastic pots (6 cubic litres; three individuals per pot) containing sand and loam (2:1) and sub-irrigated with ½ strength Hoagland nutrient solution (modified after Epstein, 1972). Plants were grown in a netted greenhouse under ambient environmental conditions (temperature: 37 ± 1 °C; relative humidity: 50 ± 5%; light intensity: 450 ± 10 μmol m^{-2} s^{-1}, photoperiod: 12 h light-12 h dark). Salinity treatments were started after thirty days of seedling acclimatization. Plants were divided into three salt treatment groups: 0, 100, 300 mM NaCl (100 plants per group) and four sub-groups: 0, 7, 15, 30 days (25 plants per sub-group). In order to avoid osmotic shock, NaCl was applied gradually with an increase of 50 mM per day in the nutrient solution. Treatment solution was completely replaced at weekly intervals until the end of the experiment.

2.2. Growth parameters

Plants were harvested after 0, 7, 15 and 30 days from each salinity treatment. The fresh weight (FW) and dry weight (DW) of each plant was determined. Freshly collected samples were cleaned and placed in an oven at 60 °C to determine the DW. Leaf area was calculated using Image J software (1.47 V). The relative growth rate (RGR; g g^{-1} d^{-1}) was calculated using the software tool of Hunt et al. (2002).

$$RGR = ULR \times LAR$$

$$LAR = SLA \times LMF$$

ULR: unit leaf rate, LAR: leaf area ratio, SLA: specific leaf area and LMF: leaf mass fraction.

Unit leaf rate (ULR): rate of increase of total dry weight per unit of total leaf area.

$$ULR\ (g\ m^{-2}\ d^{-1}) = (1/LA\ /dW/dt)$$

Leaf area ratio (LAR): ratio between the total leaf area and the total plant dry weight.

$$LAR\ (m^2\ g^{-1}) = (LA/W)$$

Leaf mass fraction (LMF): ratio between the total leaf dry weight and the total plant dry weight.

$$LMF\ (g\ g^{-1}) = (LW/W)$$

Specific leaf area (SLA): mean area of leaf displayed per unit of leaf weight.

$$SLA = (LA/LW)\ (m^2\ g^{-1})$$

2.3. Leaf gas exchange

Photosynthetic measurements were conducted on fully expended leaves (from the second node) at 7, 15 and 30 days of salinity treatment. A standard leaf chamber (2 × 3 cm^2) fitted on a portable photosynthesis system (6400XT, Li-Cor Inc., Lincoln, NE, USA) was used at ambient relative humidity: 50–60%; CO_2: 400 μmol m^{-2} s^{-1}; flow rate: 300 μmol s^{-1}; vapour pressure deficit < 2 and photosynthetically active radiation (PAR): 700 μmol m^{-2} s^{-1}. Each leaf was allowed sufficient time for equilibration in the chamber until constant readings were obtained. Instantaneous water use efficiency (WUE) was calculated as $WUE = A_{NET} / E$, and the instantaneous carboxylation efficiency as A_{NET}/Ci according to Sales et al. (2015).

2.4. Chlorophyll fluorescence

Chlorophyll fluorescence was measured on fully expanded leaves using a Pulse modulated chlorophyll fluorescence meter (2500 PAM, Walz, Germany). Leaves were dark adapted (30 min for mid-day measurements and over-night for pre-dawn measurements) before applying modulated light (< 0.1 μmol m^{-2} s^{-1}) to measure minimal fluorescence (F_0) followed by a saturating pulse of 10,000 μmol m^{-2} s^{-1} for 0.6 s to measure the maximal fluorescence (Fm). Maximum photochemical quantum yield of PSII was calculated using the formula: Fv/

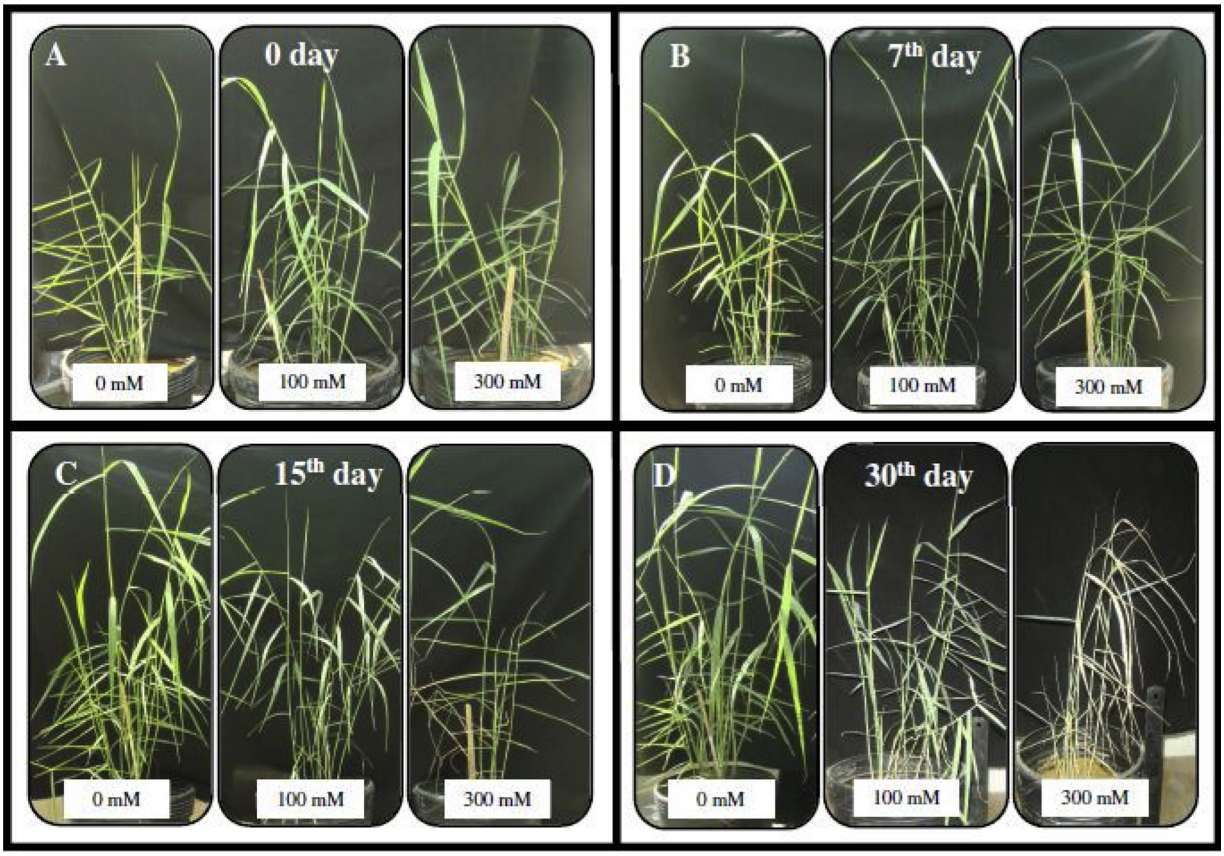

Fig. 1. Changes in morphology of *Phragmites karka* plants treated with 0, 100 and 300 mM NaCl for different time periods: 0 day (A), 7 days (B), 15 days (C) and 30 days (D).

Fm = (Fm - F_0)/Fm (Kitajima and Butler, 1975). Leaves were continuously illuminated with actinic light to measure steady-state (Fs) and maximal fluorescence (Fm') in light adapted conditions. Minimal fluorescence (F_0) was estimated using the method of Baker and Rosenqvist (2004). Effective photochemical quantum yield of PSII was calculated as Y(II) = (Fm′ - Fs)/Fm'. Quantum yield of non-regulated non-photochemical energy loss in PSII was calculated as Y(NO) = Fs/Fm and quantum yield of regulated non-photochemical energy loss in PS II was calculated as Y(NPQ) = (Fs/Fm') - (Fs/Fm) (Genty et al., 1989). Stern-Volmer type non-photochemical quenching (NPQ) was calculated as NPQ = (Fm/Fm') - 1 (Genty et al., 1989). The coefficient of photochemical quenching (qP) was calculated as (Fm'-Fs)/(Fm'-F_0) (Van Kooten and Snel, 1990). Electron transport rate (ETR) was measured by using the actual leaf absorbance values (Krall and Edwards, 1992), with the help of a LiCor integrating sphere (Li 1800-12, LiCor Inc., USA). The risk of oxidative stress was assessed by the ETR/A_{gross} ratio (Geissler et al., 2015). The indicator of light stress is given by the ratio (1-qP)/NPQ (Park et al., 1996). The photorespiration rate (P_R) was calculated using the following equation as described in Bagard et al. (2008).

$$P_R = 1/12\ [ETR - 4\ (A + Rd)]$$

2.5. Rapid light curve

Rapid light curve (RLC) measurements in dark adapted leaves were made using a Pulse modulated chlorophyll fluorescence meter (2500 PAM, Walz, Germany). Each RLC exposed the leaf to initial quasi darkness for 5–10 second, then provided a first saturating pulse followed by nine steps of increasing actinic irradiance ranging from 0 to 1800 µmol photons m^{-2} s^{-1} of 10 s duration, which finishes with a saturating pulse after each step. RLC records Y(II), Y(NPQ), Y(NO), and ETR, which can be plotted as a function of PAR irradiance. The RLCs were analyzed by non-linear regression to obtain the following parameters: maximum electron transport rate (ETR_{max}), saturating irradiance (E_s), and light harvesting efficiency of photosynthesis (α) (Statton et al., 2018).

2.6. Chlorophyll content

Content of chlorophyll *a* (Chl_a), chlorophyll *b* (Chl_b), total chlorophyll (Chl_t) and total carotenoid (C_{x+c}) were analysed using the protocol of Shabala et al. (1998). Fresh leaves were extracted with acetone (1:20) and incubated at 4 °C for 48 h. After incubation, absorbance was measured at 470, 644 and 662 nm with a spectrophotometer. Levels of Chl_a, Chl_b, Chl_t and C_{x+c} were calculated using these formulas:

$$Chl_a = 9.784\ D662 - 0.99\ D644$$

$$Chl_b = 21.42\ D644 - 4.65\ D662$$

$$Chlt = Chla + Chlb$$

$$Cx+c = (1000\ D470 - 63.14\ chlb)/214$$

2.7. Soluble sugar

Total soluble sugars were analysed by the method of Yemm and Willis (1954), using a glucose standard. Distilled water was used to extract the dried leaf samples at 100 °C for 1 h. The extract (1 ml) was mixed with (2 ml) anthrone before heating the mixture for 11 min in a boiling water bath. The reaction was stopped in an ice bath and absorbance was recorded at 630 nm.

Table 1
Relative growth rate (RGR), unit leaf rate (ULR), leaf area ratio (LAR), leaf mass fraction (LMF), and specific leaf area (SLA) of *Phragmites karka* treated with 0, 100 and 300 mM NaCl for different time durations (0–15 and 15–30 days). Similar capital letters within each salinity treatment (among time periods) and small letters among salinity treatments (within each time period) are not significantly different ($P < 0.05$) from each other, LSD test.

Salinity duration (days)	NaCl (mM)		
	0	100	300
RGR ($g\ g^{-1}\ d^{-1}$)			
0-7	0.05 ± 0.01^{Ba}	0.05 ± 0.01^{Ba}	0.02 ± 0.00^{Ab}
7-15	0.05 ± 0.01^{Ba}	0.04 ± 0.01^{Ba}	0.02 ± 0.00^{Ab}
15-30	0.14 ± 0.00^{Aa}	0.10 ± 0.00^{Ab}	0.03 ± 0.00^{Ac}
ULR ($g\ m^{-2}\ d^{-1}$)			
0-7	4.45 ± 0.23^{Ba}	3.91 ± 0.91^{Ba}	2.70 ± 0.23^{Bb}
7-15	4.40 ± 1.00^{Ba}	3.56 ± 1.12^{Ba}	1.14 ± 0.03^{Bb}
15-30	14.74 ± 1.50^{Aa}	14.40 ± 1.10^{Aa}	8.35 ± 1.30^{Ab}
LAR ($m^2\ kg^{-1}$)			
0-7	11.46 ± 2.18^{Aa}	12.24 ± 1.26^{Aa}	10.76 ± 2.93^{Aa}
7-15	10.31 ± 2.59^{Aa}	9.90 ± 0.97^{Aa}	10.20 ± 1.51^{Aa}
15-30	9.70 ± 0.40^{Aa}	7.02 ± 0.30^{Bb}	5.70 ± 0.70^{Bc}
LMF ($g\ g^{-1}$)			
0-7	0.35 ± 0.07^{Aa}	0.33 ± 0.03^{Aa}	0.33 ± 0.04^{Aa}
7-15	0.34 ± 0.09^{Aa}	0.32 ± 0.03^{Aa}	0.32 ± 0.03^{Aa}
15-30	0.34 ± 0.00^{Aa}	0.34 ± 0.00^{Aa}	0.25 ± 0.00^{Bb}
SLA ($m^2\ g^{-1}$)			
0-7	0.04 ± 0.00^{Aa}	0.04 ± 0.00^{Aa}	0.03 ± 0.01^{Aa}
7-15	0.04 ± 0.00^{Aa}	0.03 ± 0.00^{ABa}	0.03 ± 0.00^{Aa}
15-30	0.04 ± 0.00^{Aa}	0.02 ± 0.00^{Bb}	0.02 ± 0.00^{Ab}
LA (cm^2)			
7	84 ± 3.1^{Ba}	89 ± 6.00^{Ba}	40 ± 9.00^{Ab}
15	109 ± 19.2^{Ba}	81 ± 6.70^{Ba}	50 ± 4.00^{Ab}
30	703 ± 46.1^{Aa}	265 ± 14.50^{Ab}	51 ± 8.70^{Ac}

2.8. Statistical analysis

All data were examined in at least five replicates (n = 5). Statistical analysis and correlation between the various measured parameters were carried out using SPSS version 16.0 (SPSS Inc., Chicago, IL, USA). The data were analyzed using analysis of variance (ANOVA) to identify significant effects of NaCl concentration and the duration of the experiment at $P < 0.05$. LSD was used to compare individual means. Sigmaplot version 11.0 (Systat Software, San Jose, CA, USA) was used to construct graphs.

3. Results

3.1. Effect of NaCl concentration and duration on growth parameters

Plant growth and relative growth rate (RGR) of *P. karka* were significantly increased after 15 days under non-saline conditions (Fig. 1; Table 1). The relative growth rate was reduced earlier (0–7 days) at high salinity (300 mM NaCl) than at moderate salinity (100 mM NaCl). Salinity decreased leaf area (LA) and unit leaf rate (ULR) from the early phase (0–7 days) of 300 mM NaCl grown plants. Whereas, long term exposure of 300 mM NaCl reduced leaf mass fraction (LMF), specific leaf area (SLA) and leaf area ratio (LAR). However, long term exposure of moderate salinity decreased RGR due to a reduction in LAR and SLA (Table 1).

3.2. Effect of NaCl concentration and duration on leaf gas exchange parameters

Net photosynthesis (A_{NET}) decreased in non-saline control plants after 15 days. In addition, A_{NET} was unchanged in plants treated with moderate salinity compared to non-saline controls, while it started to decline linearly from the 7th day at high salinity (Fig. 2). Moderate salinity stimulated dark respiration (Rd) with time (Fig. 2). Both stomatal conductance (gs) and transpiration (E) were reduced early (7th day) at 300 mM NaCl but declined from the 15th day in 100 mM NaCl treatment (Fig. 2). Maximum WUE was found at 7 days of 300 mM NaCl treatment, which decreased with further increase in the duration of salinity treatment (Fig. 2). However, WUE increased in moderate salinity at the 30th day while it decreased in the non-saline control after 15 days. Intercellular CO_2 (Ci) declined early at 300 mM NaCl and increased gradually with time and showed a similar value as the control at the end of the experiment. However, Ci decreased in plants grown with 100 mM NaCl after 15 days of salinity treatment. Carboxylation efficiency started to decline after 15 days at 0 and 300 mM NaCl, while maximum COE (25% increase than the control) was found in plants exposed to 100 mM NaCl for long period (Fig. 2).

3.3. Effect of NaCl concentration and duration on chlorophyll fluorescence

Potential quantum yield (Fv/Fm) at mid-day and actual yield of PSII: Y(II) substantially decreased, while photoinhibition increased in plants treated with 300 mM NaCl at the 15th day (Fig. 3). However, Fv/Fm at pre-dawn decreased at 300 mM NaCl at the 30th day (Fig. 3). Chlorophyll fluorescence parameters such as Y(NO) and qP were not altered by salinity (Fig. 4). High salinity increased Y(NPQ), NPQ, the ETR/A_{gross} ratio, and $P_{R,}$ but decreased ETR and (1-qP)/NPQ (Fig. 4).

Y(II) yield decreased with increasing irradiance and the decline was more rapid in 300 mM NaCl (Fig. 5). Y(NO) was not affected by salinity and increasing irradiance. However, Y(NPQ) and NPQ increased from 100 unit of PAR in 300 mM and from 400 unit of PAR in both control and 100 mM NaCl grown plants (Fig. 5). The coefficient of photochemical quenching (qP) decreased from 600 unit of PAR in 300 mM NaCl whereas it remained similar in control and 100 mM NaCl grown plants (Fig. 5). Light harvesting efficiency of photosynthesis (α) decreased with an increase in salinity (Table 2). Whereas, maximum electron transport rate (ETR_{max}) and photosynthetic light saturating level (E_s) were highest in 100 mM NaCl, and decreased with a further increase in salinity (Fig. 5; Table 2).

3.4. Effect of NaCl concentration and duration on photosynthetic pigments

Total chlorophyll (Chl_t), Chl_a, and Chl_b content significantly increased under saline conditions from the 7th day, whereas chlorophyll content decreased at the 30th day in the non-saline control (Fig. 6). Carotenoid content increased from the 7th day in 300 mM NaCl and at the 30th day in 100 mM NaCl (Fig. 6).

3.5. Effect of NaCl concentration and duration on soluble sugar

Soluble sugar (SS) increased early (0–7 days) in plants grown with 300 mM NaCl and then decreased at the end of the experiment. However, SS increased gradually with time in moderate salinity (Fig. 7). Analysis showed significant positive correlation among various growth parameters and whole plant photosynthesis. In addition, CO_2 assimilation rate is also positively correlated with gas exchange and fluorescence parameters (Supplementary Table 1).

4. Discussion

Growth, physiological and biochemical responses of plants vary with intensity and duration of salt stress (Rakhmankulova et al., 2016; Sanchez et al., 2016; Fall et al., 2017; Pompeiano et al., 2017). Plant growth rate is strongly linked with the alteration in photosynthesis resulting from salinity (Nackley and Kim, 2015; Wungrampha et al., 2018). However, whether this reduction in photosynthesis is the reason or the result of growth reduction is not known (Abogadallah, 2010). In this study the short- and long- term impact of salinity on growth and photosynthesis were determined in a giant grass, *Phragmites karka.* Relative growth rate of *Phragmites karka* was similar in the non-saline

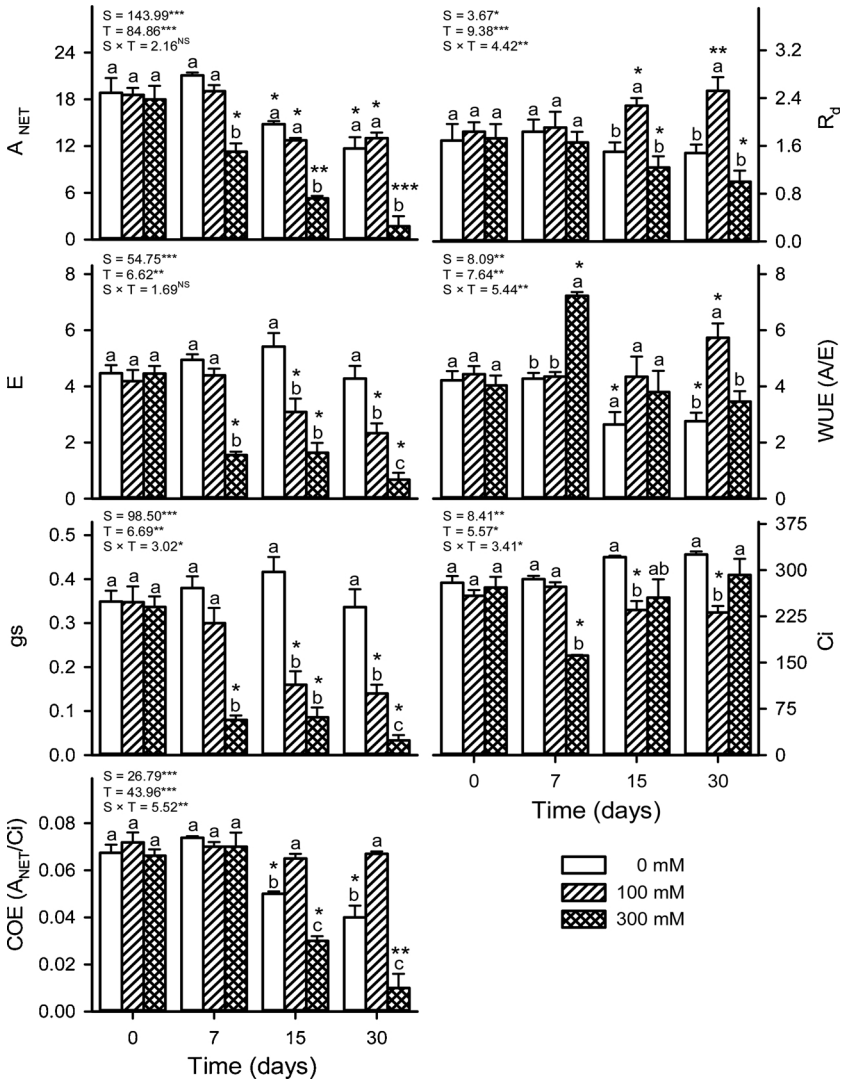

Fig. 2. Net photosynthesis ($A_{NET:}$ μmol $CO_2\,m^{-2}\,s^{-1}$), respiration (Rd: μmol $m^{-2}\,s^{-1}$), transpiration (E: mmol $m^{-2}\,s^{-1}$), water use efficiency (WUE: μmol $CO_2\,mol^{-1}\,H_2O$), stomatal conductance (gs: mol $m^{-2}\,s^{-1}$), intercellular carbon dioxide concentration (Ci: μmol $m^{-2}\,s^{-1}$), and instantaneous carboxylation efficiency (COE: A_{NET}/Ci) of *Phragmites karka* after 0, 100 and 300 mM NaCl treatments at 7, 15 and 30 days. *F* and *P* (*** $P < 0.001$, ** $P < 0.01$, * $P < 0.05$, ns = non-significant) values of the two-way ANOVAs are presented, S: salinity, T: time and T × S: time × salinity interaction. For each time period, values among salinity treatments with different LSD letters represent significant differences at $P < 0.05$. Asterisks indicate significant differences among time periods at each NaCl treatment.

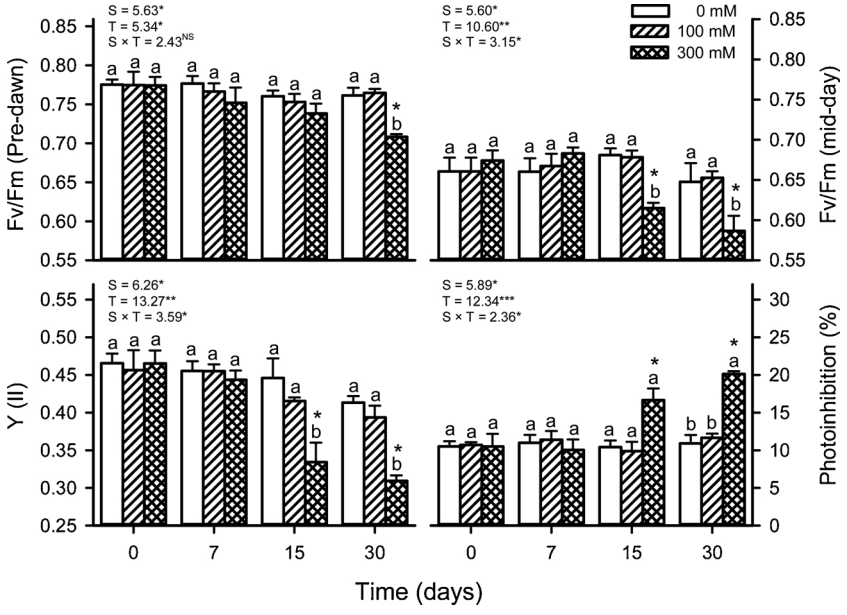

Fig. 3. Maximum quantum yield of PSII: Fv/Fm (Pre-dawn and Mid-day), actual yield of PSII: Y(II) and photoinhibition of *Phragmites karka* after 0, 100 and 300 mM NaCl treatments at 7, 15 and 30 days. *F* and *P* (*** $P < 0.001$, ** $P < 0.01$, * $P < 0.05$, ns = non-significant) values of the two-way ANOVAs are presented, S: salinity, T: time and T × S: time × salinity interaction. For each time period, values among salinity treatments with different LSD letters represent significant differences at $P < 0.05$. Asterisks indicate significant differences among time periods at each NaCl treatment.

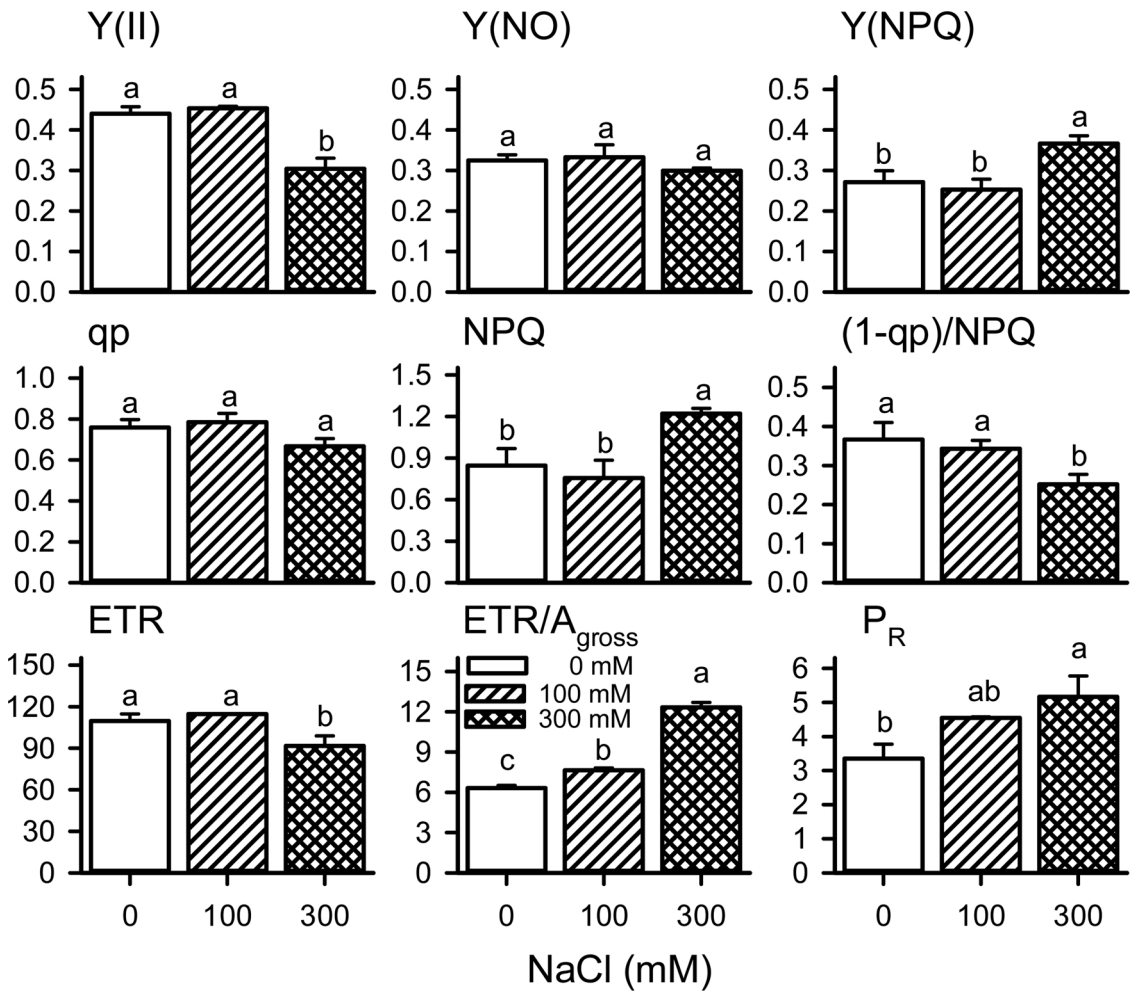

Fig. 4. Effective photochemical quantum yield of PSII: Y(II), quantum yield of non-regulated non-photochemical energy loss in PSII: Y(NO), quantum yield of regulated non-photochemical energy loss in PSII: Y(NPQ), photochemical quenching (qP), non-photochemical quenching (NPQ), indicator of light stress (1-qp)/NPQ, electron transport rate (ETR), risk of oxidative stress (ETR/A_{gross}) and photorespiration rate (P_R) of *Phragmites karka* after 0, 100 and 300 mM NaCl treatments for 15 days. Values among salinity treatments with different LSD letters represent significant differences at $P < 0.05$.

control and 100 mM NaCl treated plants until the 15th day; however, from 15 to 30 days a fast growth rate was observed, which represents optimal growth in the absence of salinity. Rapid plant growth in non-saline conditions was significantly correlated with whole plant photosynthesis (r = 0.760) (Supplementary Table 1). Abideen et al. (2014) previously reported growth stimulation in *P. karka* under moderate salinity, which seems to be the result of differences in plant environmental conditions (temperature, humidity, light intensity) and experimental setup (use of quick check system for periodic flooding-twice a day). However, in this study *P. karka* was grown similarly to natural field environmental conditions with a sub-irrigation system. Relative growth rate decreased at high salinity during early treatment (0–7 days) of salinity. Salinity induced reduction in growth rate has been reported in many halophytic grasses such as *Phragmites communis* (Gorai et al., 2007); *Phragmites australis* (Gorai et al., 2011); *Halodule uninervis* (Khalafallah et al., 2013); *Aeluropus lagopoides*, *Sporobolus tremulus*, *Paspalum paspalodes*, and *Paspalidium germinatum* (Moinuddin et al., 2014). In this experiment, RGR is positively correlated with unit leaf rate (ULR: r = 0.897), as well as biomass allocated to leaf area (LAR: r = 0.751, supplementary Table1), indicating the role of both leaf biomass and assimilation per unit area in regulating the growth rate. However, RGR dependence on ULR and LAR varies with intensity and time of exposure with salinity. Relative growth rate decreased at 300 mM NaCl within 7 days due to a decline in the ULR, which was also supported by the data from the net photosynthesis rate. However, after 15 days exposure to 100 mM NaCl, RGR decreased due to a reduction in biomass allocated to leaf area (decreased LAR) rather than ULR. The leaf area ratio depends on both SLA (leaf area per unit leaf dry mass; r = 0.871) and LMF (total leaf dry weight per total plant dry weight; r = 0.953) (supplementary Table 1), however this dependence varies with increasing salinity concentration. A reduction in LAR after prolonged exposure at 100 mM NaCl was linked with the development of smaller and thicker leaves (decreased SLA). The decrease in growth rate due to a reduction in LAR and SLA under salinity has also been reported in grasses like *Phragmites australis* (Eller et al., 2014); *Arundo donax,* and *Panicum virgatum* (Sanchez et al., 2016). The decrease in RGR during prolonged exposure to 300 mM was attributed to both ULR and LAR. Lower LAR was due to a decrease in leaf mass fraction (LMF) and SLA at high salinity which shows the existence of variation in leaf plasticity of *P. karka* to survive in saline areas for longer periods. Salinity stress alters photosynthesis directly due to stomatal-mesophyll limitations and/or biochemical restrictions (photochemical or oxidative damage) (Asrar et al., 2017; Moinuddin et al., 2017; Wungrampha et al., 2018). Stomatal regulation and CO_2 fixation vary with plant species and duration of salt exposure (Liu et al., 2011; Yan et al., 2015). Net photosynthesis of plants was maintained in 100 mM NaCl while a considerable (2-fold) decrease was noted in 300 mM at the 7th day compared to the control plants. Reduction in photosynthesis at high salinity was linked with lower stomatal conductance (gs) and intercellular carbon dioxide concentration (Ci). However, carboxylation efficiency

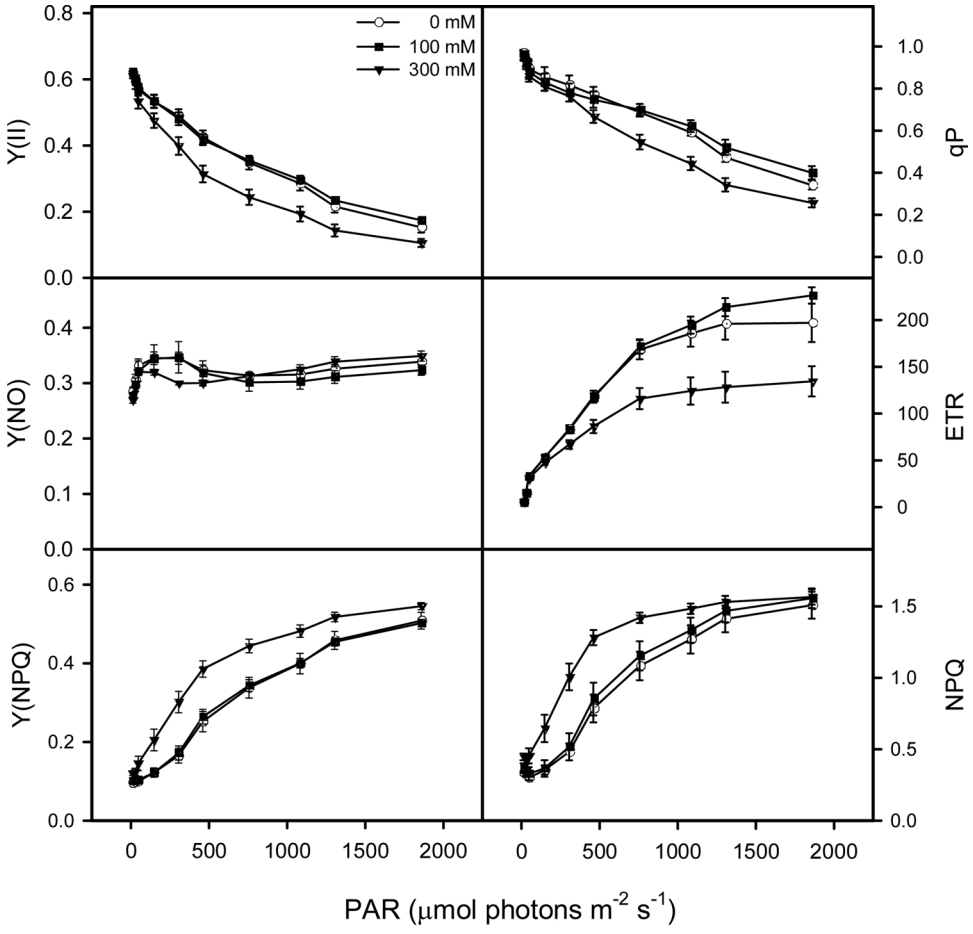

Fig. 5. Effective photochemical quantum yield of PSII: Y(II), quantum yield of non-regulated non-photochemical energy loss in PSII: Y(NO), quantum yield of regulated non-photochemical energy loss in PSII: Y(NPQ), photochemical quenching (qP), electron transport rate (ETR), and non-photochemical quenching (NPQ) as a function of photosynthetic active rediation (PAR) of *Phragmites karka* after 0, 100 and 300 mM NaCl treatments for 15 days.

Table 2
Maximum electron transport rate (ETR_{max}), photosynthetic light saturating level (E_s) and light harvesting efficiency of photosynthesis (α) derived from rapid light curve of *Phragmites karka* after 0, 100 and 300 mM NaCl treatments for 15 days. Values among salinity treatments with different LSD letters represent significant differences at $P < 0.05$.

Parameters	NaCl (mM)		
	0	100	300
ETR_{max} (electrons m^{-2} s^{-1})	211.15 ± 6.3^{b}	248.68 ± 5.1^{a}	136.80 ± 4.6^{c}
E_s (mol m^{-2} s^{-1})	1265.48 ± 14.9^{b}	1624.68 ± 18.4^{a}	1015.21 ± 12.1^{c}
α (electron/photon)	0.38 ± 0.0^{a}	0.35 ± 0.0^{b}	0.30 ± 0.0^{c}

(COE) was unaffected in the early phase of high salinity which indicates that the reduction in photosynthesis was initiated by stomatal limitation. Decreased stomatal conductance resulted in lower transpiration in the first 7 days of high salinity that helps plants to prevent water loss and enhance water use efficiency, which is a known trait of salt resistance grasses in saline conditions (Nackley and Kim, 2015; Webster et al., 2016). However, a decline in gs also leads to a decrease in Ci and ultimately photosynthesis (Liu et al., 2011). After long term exposure to moderate salinity, plants increased photosynthetic light saturating levels (E_s) to utilize maximum light for photosynthesis, also indicated by increased maximum electron transport rate that resulted in the maintenance of net assimilation rate (A_{Net}) similar to control plants. Moreover, increases in mesophyll thickness (lower SLA) could maximize internal surface area for CO_2 absorption and improve net photosynthesis rate per leaf area (Nackley and Kim, 2015). The enhanced carboxylation efficiency (COE) (1.5-fold) also helps to maintain the net assimilation rate at moderate salinity. However, after long term exposure to high salinity, net photosynthesis decreased along with a reduction in gs while Ci was maintained. In addition, instantaneous carboxylation efficiency significantly decreased (4-fold than controls), representing both stomatal and biochemical limitations of photosynthesis in the later phase of 300 mM NaCl treatment. Our results showed a positive correlation among CO_2 assimilation rate (A_{NET}) and gas exchange parameters (gs: r = 0.794; COE: r = 0.896), indicating the role of both stomatal and biochemical limitation in regulating A_{NET} under high salinity (Supplementary Table 1). Similar results were also reported in some halophytic grasses where stomatal factor limits photosynthesis under short term salinity stress, but prolonged exposure caused both stomatal and biochemical limitation (Liu et al., 2011; Yan et al., 2015).

A higher energy demand to respond to moderate salinity increases the accumulation of soluble sugar (possibly for osmotic adjustment and ROS defence mechanisms) and the rate of respiration (1.5-fold than control) that caused a deficiency of C-skeleton and inhibition of leaf growth (Kumar et al., 2016; Rakhmankulova et al., 2016; Sami et al., 2016). An increased content of soluble sugar under salinity was observed in the halophytic grasses *Paspalidium geminatum* (Moinuddin et al., 2014); *Aeluropus lagopoides* (Kumar et al., 2016); and *Paspalum vaginatum* (Pompeiano et al., 2016). Moreover, soluble sugar accumulation, 2-fold compared to non-saline controls, with 300 mM NaCl treatment could cause feedback inhibition of photosynthesis (Dadkhah and Rassam, 2016).

The maximum quantum efficiency of PSII (Fv/Fm) not only measures the instantaneous photosynthetic capacity of a plant but also indicates photoinhibition or salt induced damage to PSII as the difference of pre-dawn and mid-day values (Yan et al., 2015). In *P. karka*, the mid-day Fv/Fm value significantly ($P <$ 0.05) decreased after 15 days exposure to 300 mM NaCl. Whereas, the reduction in mid-day Fv/Fm

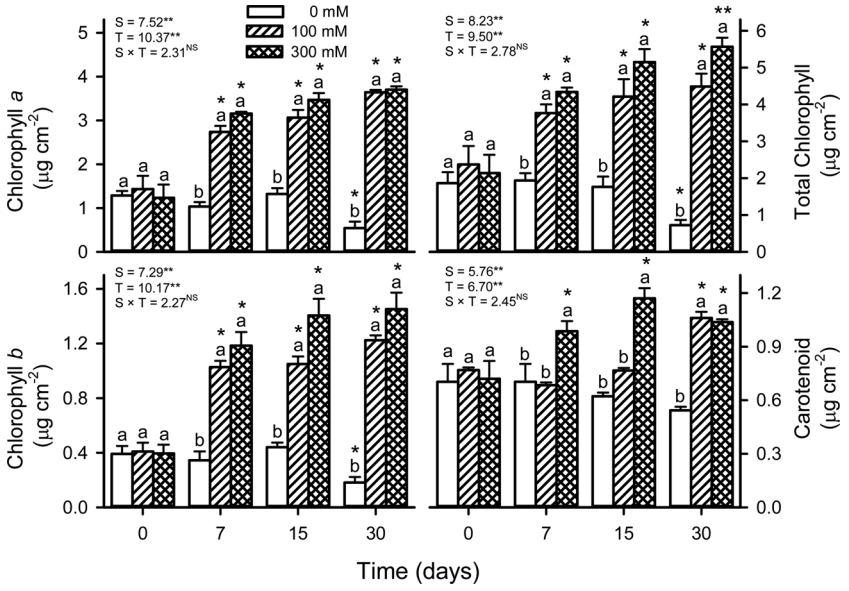

Fig. 6. Chlorophyll and carotenoid content of *Phragmites karka* after 0, 100 and 300 mM NaCl treatments at 7, 15 and 30 days. *F* and *P* (** $P <$ 0.01, ns = non-significant) values of the two-way ANOVAs are presented, S: salinity, T: time and T × S: time × salinity interaction. For each time period, values among salinity treatments with different LSD letters represent significant differences at $P < 0.05$. Asterisks indicate significant differences among time periods at each NaCl treatment.

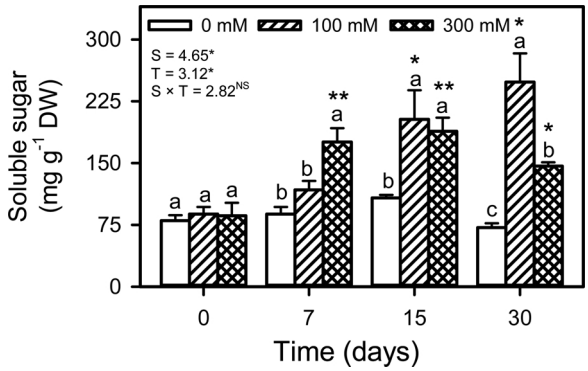

Fig. 7. Soluble sugar of *Phragmites karka* after 0, 100 and 300 mM NaCl treatments at 7, 15 and 30 days. *F* and *P* (* $P <$ 0.05, ns = non-significant) values of the two-way ANOVAs are presented, S: salinity, T: time and T × S: time × salinity interaction. For each time period, values among salinity treatments with different LSD letters represent significant differences at $P < 0.05$. Asterisks indicate significant differences among time periods at each NaCl treatment.

value completely recovered during the overnight period by dawn value, indicating dynamic photoinhibition (Qiu et al., 2003). The decline in mid-day Fv/Fm under high salinity at 15 days could be a way to down-regulate the light harvesting reaction [decreased Y(II)] and thus not the consequence of photo-damage (Qiu et al., 2003; Yan et al., 2015). However, the mid-day and predawn Fv/Fm values both decreased at the 30th day of exposure to 300 mM NaCl, indicating chronic photoinhibition (Qiu et al., 2003). Our results also indicate a positive correlation of fluorescence parameters Fv/Fm and Y(II) with CO_2 assimilation rate (Supplementary Table 1).

Chlorophyll and carotenoids are light harvesting components of the photosynthetic apparatus. Salt stress is reported to cause chlorophyll destruction in many halophytic grasses; however, in some species increased chlorophyll content under salinity could be linked with plant salt tolerance (Stefanov et al., 2016). In this study, chlorophyll content decreased with time in the non-saline control; however, it increased from the early phase under saline conditions. In non-saline conditions, *P. karka* sharply increased photosynthetic active tissues (leaf number and leaf area) after two weeks, which correlated with a decrease in all photosynthetic pigments (Chlorophyll and carotenoids) and low photosynthesis (A_{NET}) on a unit leaf area basis, as previously reported in other halophytic grasses: *Eremochloa ophiuroides* (Liu et al., 2011), *Arundo donax* and *Panicum virgatum* (Sanchez et al., 2016). This indicated that the reduction in A_{NET} after 15 days under non-saline condition was not due to stomatal limitation (as no change in E and Ci), water limitation (as lower WUE) and photosystem damage (no change in Fv/Fm, YII and photoinhibition). However, the substantial increase in leaf area after 15 days under control conditions was directly linked with whole plant photosynthesis. Higher chlorophyll content in *P. karka* under salinity could be related to both increased thylakoid number per chloroplast and enhanced mesophyll thickness (lower SLA) (Pompeiano et al., 2016). In addition, higher chlorophyll content helps plants to increase light absorption at 100 mM NaCl, which functions to retain the photosynthesis rate similar to controls. However, carotenoid content increases in the later phase of moderate salinity possibly prevent formation of singlet oxygen (Asrar et al., 2017). Salt stress-induced increases in chlorophyll and carotenoid content to support photosynthesis were also reported in some halophytic grasses: *Zoysia japonica* (Pompeiano et al., 2014); *Paspalum vaginatum* (Pompeiano et al., 2016); and *Paspalum scrobiculatum* (Shonubi and Okusanya, 2007). However, under high salinity increased chlorophyll content can enhance the flow of electrons through the photosystems, which increases the risk of photoinhibition. Under high salinity plants cannot cope with excess light due to salinity as an indicator that light stress (1-qP)/NPQ ratio increased, resulting in an increased risk of oxidative stress (ETR/Agross). Excess light energy could enhance reactive oxygen species synthesis, which causes damage to chloroplasts at the cellular level (Yordanova and Popova, 2007). Plants can dissipate excess energy either by photochemical or non-photochemical quenching (Moinuddin et al., 2017). In high salinity, photochemical quenching (qP) remained the same, whereas the fraction of absorbed light used in photochemistry Y(II) and ETR decreased. The reduction in maximum electron transport rate (ETR_{max})and light harvesting efficiency of photosynthesis (α) at 300 mM NaCl could be linked with the reduction in net assimilation rate, and ultimately biomass production, this led to increased carbon demand as previously reported in *P. australis* (Eller et al., 2014). This indicated that the excessive electrons that run through the PS II could not be used in electron transport, so they are either used in non-photochemical quenching or they could be stored as alternative electron sinks through the Mehler reaction, photorespiration or cyclic electron transport (Takahashi et al., 2008). High salinity plants use a regulated and efficient process Y(NPQ) to dissipate absorbed light energy in the form of heat, so quantum yield loss by non-regulated process Y(NO) remained unchanged. A similar result has been reported in other halophytic grasses such as *Paspalum paspalodes* and *Paspalidium geminatum* (Moinuddin et al., 2017). Plants increased carotenoid content from the

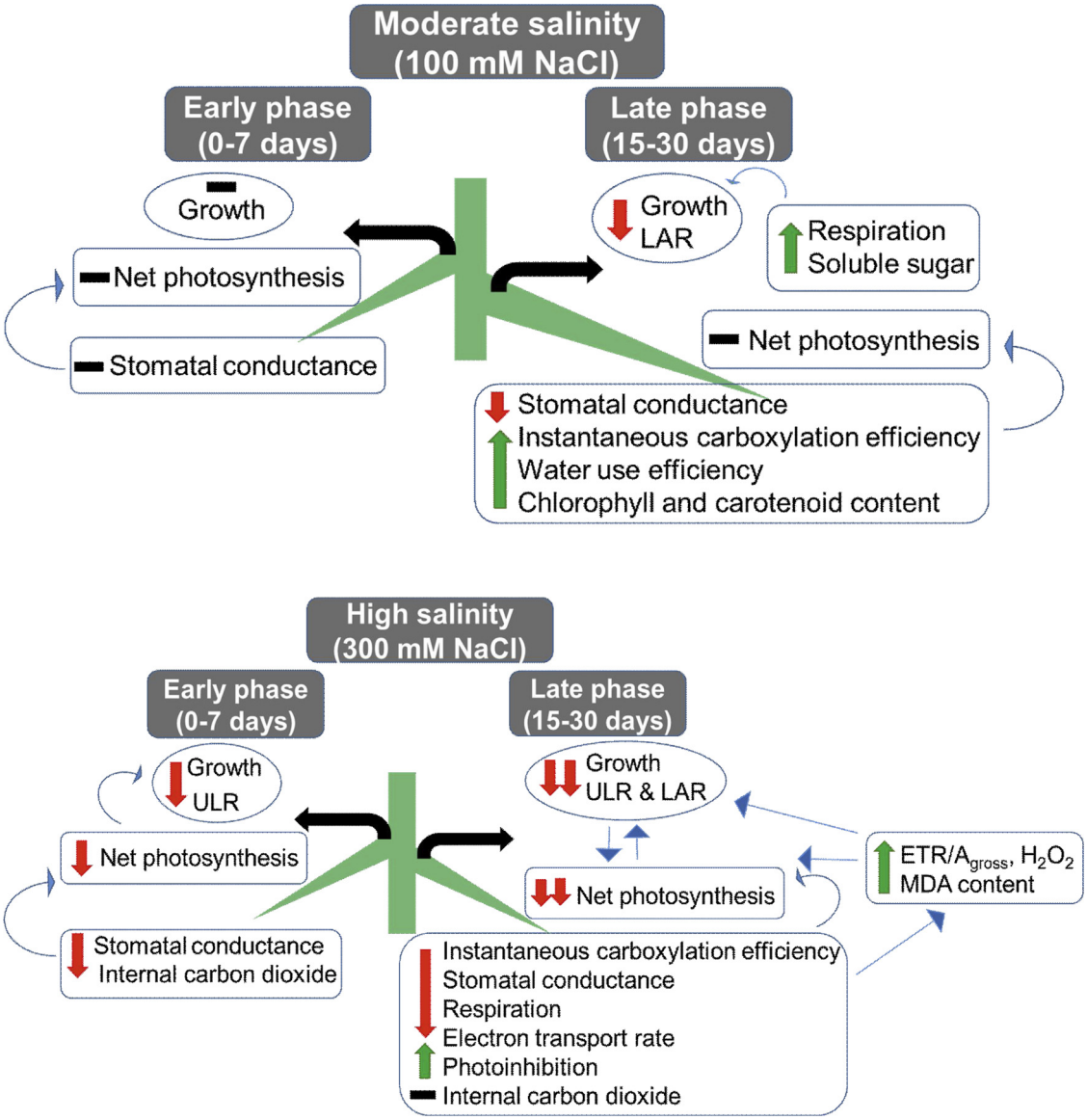

Fig. 8. Schematic model representing changes in growth and gas exchange parameters of *Phragmites karka* grown with 100 and 300 mM NaCl treatments. The direction of the arrow shows the change (green upward arrow: increase; red downward arrow: decrease) in comparison with non-saline grown plants while the number of arrows represents significant differences ($P < 0.05$) between salinity treatments. Dashed black lines represent no change from the control (For interpretation of the references to colour in this figure legend, the reader is referred to the web version of this article).
Abbreviations: Leaf area ratio (LAR), unit leaf rate (ULR), hydrogen peroxide (H_2O_2), maondialdehyde (MDA).

early phase of high salinity that contributes to regulated photo-protective NPQ to dissipate energy in the form of heat via the xanthophyll cycle (Pompeiano et al., 2017; Moinuddin et al., 2017). However, long term (30 days) exposure to high salinity also increased photorespiration to sustain photons in a non-assimilatory pathway, which thus functions as a sink for excessive excitation energy (Lima et al., 2017). The coordination between photochemistry and alternate electron sink (xanthophyll cycle, photo-protective compound carotenoidsand photorespiration) can assist plants to avoid damage to the photosystems (Qiu et al., 2003; Lima et al., 2017; Moinuddin et al., 2017; Pompeiano et al., 2017). However, these modifications could not completely protect the plant from high salinity during long term exposure.

5. Conclusion

In conclusion, *Phragmites karka* maintains relative growth rate (RGR) during the early phase of moderate salinity treatment, which decreased at high salinity due to a reduction in unit leaf rate (ULR). However, in the later phase, decreased RGR at moderate salinity was the result of lower leaf area ratio (LAR), whereas at high salinity the reduction in RGR was the consequence of both ULR and LAR. *Phragmites karka* under moderate salinity maintained net photosynthesis through increased chlorophyll content, and improved water use and carboxylation efficiency (Fig. 8). Moreover, photo protection due to increased carotenoid content helps in maintaining PSII yield and avoiding membrane damage. Photosynthesis reduction under high salinity was due to stomatal limitation during the early phase. However, in the late phase of high salinity treatment, both stomatal and biochemical factors were responsible for the reduction in net CO_2 assimilation (Fig. 8). This study provides a detailed explanation for the impact of salt concentration and duration on biomass and photosynthesis regulation in the giant grass *P. karka*.

Author contributions

Erum Shoukat, Muhammad Zaheer Ahmed and Zainul Abideen contributed in experiment designing, interpretation of data and drafting of the article. Salman Gulzar helped in leaf gas–exchange analysis while Brent L. Nielsen contributed in critical revision of the article.

Conflicts of interest

The authors declare no conflicts of interest.

Funding

This research did not receive any specific grant from funding agencies in the public, commercial, or not-for-profit sectors.

Acknowledgements

Authors would like to thank *Dr. Hans Werner Koyro* for his guidance to shape this draft into its final form. Authors are also thankful to ISHU for internal support.

Appendix A. Supplementary data

Supplementary material related to this article can be found, in the online version, at doi:https://doi.org/10.1016/j.envexpbot.2019.03.024.

References

Abideen, Z., Ansari, R., Khan, M.A., 2011. Halophytes: potential source of ligno-cellulosic biomass for ethanol production. Biomass Bioenergy 35 (5), 1818–1822.
Abideen, Z., Koyro, H.W., Huchzermeyer, B., Ahmed, M.Z., Gul, B., Khan, M.A., 2014. Moderate salinity stimulates growth and photosynthesis of *Phragmites karka* by water relations and tissue specific ion regulation. Environ. Exp. Bot. 105, 70–76.
Abideen, Z., Qasim, M., Hussain, T., Rasheed, A., Gul, B., Koyro, H.W., Ansari, R., Khan, M.A., 2018. Salinity improves growth, photosynthesis and bioenergy characteristics of *Phragmites karka*. Crop Past. Sci. 69 (9), 944–953.
Abogadallah, G.M., 2010. Sensitivity of *Trifolium alexandrinum* L. To salt stress is related to the lack of long-term stress-induced gene expression. Plant Sci. 178, 491–500.
Asrar, H., Hussain, T., Hadi, S.M.S., Gul, B., Nielsen, B.L., Khan, M.A., 2017. Salinity induced changes in light harvesting and carbon assimilating complexes of *Desmostachya bipinnata* (L.) staph. Environ. Exp. Bot. 135, 86–95.
Bagard, M., Le Thiec, D., Delacote, E., Hasenfratz-Sauder, M.P., Banvoy, J., Gérard, J., Dizengremel, P., Jolivet, Y., 2008. Ozone-induced changes in photosynthesis and photorespiration of hybrid poplar in relation to the developmental stage of the leaves. Physiol. Plant. 134 (4), 559–574.
Baker, N.R., Rosenqvist, E., 2004. Applications of chlorophyll fluorescence can improve crop production strategies: an examination of future possibilities. J. Exp. Bot. 55 (403), 1607–1621.
Dadkhah, A., Rassam, G., 2016. Effect of salinity on photosynthesis and leaf carbohydrate content in two wheat (*Triticum aestivum* L.). Jordan J. Agric. Sci. 405 (3641), 1–12.
Eller, F., Lambertini, C., Nguyen, L.X., Brix, H., 2014. Increased invasive potential of non-native *Phragmites australis*: elevated CO2 and temperature alleviate salinity effects on photosynthesis and growth. Glob. Change Biol. 20 (2), 531–543.
Epstein, E., 1972. Mineral Nutrition of Plants: Principles and Perspectives. John Wiley and Sons, New York.
Fall, F., Diouf, D., Fall, D., Bakhoum, N., Thioye, B., Kane, A., Ndiaye, C., Ndoye, I., Bâ, A.M., 2017. Growth and physiological responses of *Sporobolus robustus* kunth seedlings to salt stress. Arid. Land Res. Manag. 31 (1), 46–56.
Flora of Pakistan, 2011. *Phragmites karka* (Retz.) Trin. ex Steud. Published. Nomenclator Botanicus. Editio Secunda 1: 144. 1840. (Nomencl. Bot. (ed. 2). . https://www.tropicos.org/Name/25509878?projectid=32.
Geissler, N., Hussin, S., El-Far, M.M., Koyro, H.W., 2015. Elevated atmospheric CO_2 concentration leads to different salt resistance mechanisms in a C_3 (*Chenopodium quinoa*) and a C_4 (*Atriplex nummularia*) halophyte. Environ. Exp. Bot. 118, 67–77.
Genty, B., Briantais, J.M., Baker, N.R., 1989. The relationship between the quantum yield of photosynthetic electron transport and quenching of chlorophyll fluorescence. Biochim. et Biophys. Acta (BBA) Gen. Sub. 990 (1), 87–92.
Gorai, M., Vadel, A.M., Neffati, M., Khemira, H., 2007. The effect of sodium chloride salinity on the growth, water status and ion content of *Phragmites communis* trin. Pak. J. Biol. Sci. 10 (13), 2225–2230.
Gorai, M., Ennajeh, M., Khemira, H., Neffati, M., 2011. Influence of NaCl-salinity on growth, photosynthesis, water relations and solute accumulation in *Phragmites australis*. Acta Physiol. Plant. 33 (3), 963–971.
Hetherington, A.M., Woodward, F.I., 2003. The role of stomata in sensing and driving environmental change. Nature 424 (6951), 901.
Hunt, R., Causton, D.R., Shipley, B., Askew, A.P., 2002. A modern tool for classical plant growth analysis. Ann. Bot. 90 (4), 485–488.
Khalafallah, A.A., Geneid, Y.A., Shaetaey, S.A., Shaaban, B., 2013. Responses of the seagrass *Halodule uninervis* (Forssk.) aschers to hypersaline conditions. Egypt. J. Aquat. Res. 39 (3), 167–176.
Kitajima, M., Butler, W.L., 1975. Quenching of chlorophyll fluorescence and primary photochemistry in chloroplasts by dibromothymoquinone. Biochim. et Biophys. Acta (BBA) Bioenerg. 376 (1), 105–115.
Krall, J.P., Edwards, G.E., 1992. Relationship between photosystem II activity and CO_2 fixation in leaves. Physiol. Plant. 86, 180–187.
Kumar, A., Kumar, A., Lata, C., Kumar, S., 2016. Eco-physiological responses of *Aeluropus lagopoides* (grass halophyte) and *Suaeda nudiflora* (non-grass halophyte) under individual and interactive sodic and salt stress. South Afr. J. Bot. 105, 36–44.
Liang, W., Ma, X., Wan, P., Liu, L., 2018. Plant salt-tolerance mechanism: a review. Biochem. Biophys. Res. Commun. 495 (1), 286–291.
Lima[nato], M.C., Cerqueira, J.V.A., Cunha, J.R.D., Ribeiro, R.V., Silveira, J.A.G., 2017. Cyclic electron flow, NPQ and photorespiration are crucial for the establishment of young plants of *Ricinus communis* and *Jatropha curcas* exposed to drought. Plant Biol. 19 (4), 650–659.
Liu, Y., Du, H., Wang, K., Huang, B., Wang, Z., 2011. Differential photosynthetic responses to salinity stress between two perennial grass species contrasting in salinity tolerance. Hortic. Sci. 46 (2), 311–316.
Megdiche, W., Hessini, K., Gharbi, F., Jaleel, C.A., Ksouri, R., Abdelly, C., 2008. Photosynthesis and photosystem II efficiency of two salt-adapted halophytic seashore *Cakile maritima* ecotypes. Photosynthetica 46, 410–419.
Millar, J., Roots, J., 2012. Changes in Australian agriculture and land use: implications for future food security. Int. J. Agric. Sustain. 10, 25–39.
Moinuddin, M., Gulzar, S., Ahmed, M.Z., Gul, B., Koyro, H.W., Khan, M.A., 2014. Excreting and non-excreting grasses exhibit different salt resistance strategies. AoB Plants 6 plu038.
Moinuddin, M., Gulzar, S., Hameed, A., Gul, B., Khan, M.A., Edwards, G.E., 2017. Differences in photosynthetic syndromes of four halophytic marsh grasses in Pakistan. Photosyn. Res. 131 (1), 51–64.
Nackley, L.L., Kim, S.H., 2015. A salt on the bioenergy and biological invasions debate: salinity tolerance of the invasive biomass feedstock *Arundo donax*. GCB Bioenergy 7 (4), 752–762.
Pang, Q., Chen, S., Dai, S., Chen, Y., Wang, Y., Yan, X., 2010. Comparative proteomics of salt tolerance in *Arabidopsis thaliana* and *Thellungiella halophila*. J. Proteome Res. 9, 2584–2599.
Park, Y.I., Chow, W.S., Anderson, J.M., 1996. Chloroplast movement in the shade plant *Tradescantia albiflora* helps protect photosystem II against light stress. Plant Physiol. 111 (3), 867–875.
Percey, W.J., McMinn, A., Bose, J., Breadmore, M.C., Guijt, R.M., Shabala, S., 2016. Salinity effects on chloroplast PSII performance in glycophytes and halophytes. Funct. Plant Biol. 43 (11), 1003–1015.
Pompeiano, A., Giannini, V., Gaetani, M., Vita, F., Guglielminetti, L., Bonari, E., Volterrani, M., 2014. Response of warm–season grasses to N fertilization and salinity. Sci. Hortic. 177, 92–98.
Pompeiano, A., Di Patrizio, E., Volterrani, M., Scartazza, A., Guglielminetti, L., 2016. Growth responses and physiological traits of seashore paspalum subjected to short-term salinity stress and recovery. *Agric. Water Manag.* 163, 57–65.
Pompeiano, A., Landi, M., Meloni, G., Vita, F., Guglielminetti, L., Guidi, L., 2017. Allocation pattern, ion partitioning, and chlorophyll *a* fluorescence in *Arundo donax* L. in responses to salinity stress. Plant Biosyst. 151 (4), 613–622.
Qiu, N., Lu, Q., Lu, C., 2003. Photosynthesis, photosystem II efficiency and the xanthophyll cycle in the salt-adapted halophyte *Atriplex centralasiatica*. New Phytol. 159 (2), 479–486.
Rakhmankulova, Z.F., Shuyskaya, E.V., Suyundukov, Y.T., Usmanov, I.Y., Voronin, P.Y., 2016. Different responses of two ecotypes of C_3–C_4 xero-halophyte *Bassia sedoides* to osmotic and ionic factors of salt stress. Russ. J. Plant Physiol. 63 (3), 349–357.
Redondo-Gómez, S., Mateos-Naranjo, E., Davy, A.J., Fernández-Muñoz, F., Castellanos, E.M., Luque, T., Figueroa, M.E., 2007. Growth and photosynthetic responses to salinity of the salt-marsh shrub *Atriplex portulacoides*. Ann. Bot. 100 (3), 555–563.
Sales, C.R., Marchiori, P.E.R., Machado, R.S., Fontenele, A.V., Machado, E.C., Silveira, J.A.G., Ribeiro, R.V., 2015. Photosynthetic and antioxidant responses to drought during sugarcane ripening. Photosynthetica 53 (4), 547–554.
Sami, F., Yusuf, M., Faizan, M., Faraz, A., Hayat, S., 2016. Role of sugars under abiotic stress. Plant Physiol. Biochem. 109, 54–61.
Sanchez, E., Gil, S., Azcón-Bieto, J., Nogués, S., 2016. The response of *Arundo donax* L. (C_3) and *Panicum virgatum* (C_4) to different stresses. Biomass Bioenergy 85, 335–345.
Shabala, S.N., Shabala, S.I., Martynenko, A.I., Babourina, O., Newman, I.A., 1998. Salinity effect on bioelectric activity, growth, Na^+ accumulation and chlorophyll fluorescence of maize leaves: a comparative survey and prospects for screening. Funct. Plant Biol. 25 (5), 609–616.
Shamsutdinov, N.Z., Shamsutdinova, E.Z., Orlovsky, N.S., Shamsutdinov, Z.S., 2017. Halophytes: ecological features, global resources, and outlook for multipurpose use. Her. Russ. Acad. Sci. 87 (1), 1–11.
Shonubi, O.O., Okusanya, O.T., 2007. The growth and physiological responses of *Paspalum vaginatum* Sw. and *Paspalum scrobiculatum* Linn. In relation to salinity. Asian J. Plant Sci. 6 (6), 949–956.
Slama, I., Abdelly, C., Bouchereau, A., Flowers, T., Savouré, A., 2015. Diversity, distribution and roles of osmoprotective compounds accumulated in halophytes under abiotic stress. Ann. Bot. 115 (3), 433–447.
Statton, J., McMahon, K., Lavery, P., Kendrick, G.A., 2018. Determining light stress responses for a tropical multi-species seagrass assemblage. Mar. Pollut. Bull. 128,

508–518.
Stefanov, M., Yotsova, E., Rashkov, G., Ivanova, K., Markovska, Y., Apostolova, E.L., 2016. Effects of salinity on the photosynthetic apparatus of two Paulownia lines. Plant Physiol. Biochem. 101, 54–59.
Takahashi, S., Badger, M.R., 2011. Photoprotection in plants: a new light on photosystem II damage. Trends Plant Sci. 16 (1), 53–60.
Van Kooten, O., Snel, J.F., 1990. The use of chlorophyll fluorescence nomenclature in plant stress physiology. Photosynth. Res. 25, 147–150.
Webster, R.J., Driever, S.M., Kromdijk, J., McGrath, J., Leakey, A.D., Siebke, B., Siebke, K., Shah, T.D., Bonnage, S., Peloe, T., Long, S.P., 2016. High C_3 photosynthetic capacity and high intrinsic water use efficiency underlies the high productivity of the bioenergy grass *Arundo donax*. Sci. Rep. 6, 20694.
Wungrampha, S., Joshi, R., Singla-Pareek, S.L., Pareek, A., 2018. Photosynthesis and salinity: are these mutually exclusive? Photosynthetica 1–16.
Yan, K., Wu, C., Zhang, L., Chen, X., 2015. Contrasting photosynthesis and photoinhibition in tetraploid and its auto diploid honeysuckle (*Lonicera japonica* Thunb.) under salt stress. Front. Plant Sci. 6, 227.
Yang, Y., Guo, Y., 2018. Elucidating the molecular mechanisms mediating plant salt-stress responses. New Phytol. 217 (2), 523–539.
Yemm, E.W., Willis, A.J., 1954. The estimation of carbohydrates in plant extracts by anthrone. Biochem. J. 57 (3), 508.
Yordanova, R.Y., Popova, L.P., 2007. Flooding-induced changes in photosynthesis and oxidative status in maize plants. Acta Physiol. Plant. 29 (6), 535–541.